CHIN. PHYS. LETT. Vol. 35, No. 3 (2018) 034201

# Designing Fano-Like Quantum Routing via Atomic Dipole-Dipole Interactions *

Jin-Song Huang(黄劲松)[1,2**], Jia-Hao Zhang(张家豪)[1], Yan Wang(王艳)[3], Zhong-Hui Xu(徐中辉)[1]

[1]*School of Information Engineering, Jiangxi University of Science and Technology, Ganzhou 341000*

[2]*Department of Physics, South China University of Technology, Guangzhou 510640*

[3]*School of Foreign Studies, Jiangxi University of Science and Technology, Ganzhou 341000*

(Received 23 October 2017)

*Fano-like quantum routing of single photons in a system with two waveguides coupled to two collocated atoms is investigated theoretically. Using a full quantum theory in real space, photonic scattering amplitudes along four ports of the waveguide network are analytically obtained. It is shown that, by adjusting the atomic dipole-dipole interaction, an evident Fano-line shape emerges in the scattering spectra of the single-dot configuration system. Moreover, Fano resonance can also be achieved by varying the atom-waveguide coupling strength and atomic detuning, in the presence of the atomic dipole-dipole interaction. Therefore, the atomic dipole-dipole interaction may be utilized as a possible way to control spectral Fano-like resonance. The feasibility with the experimental waveguide channels is also discussed.*

*PACS:* 42.50.Ct, 42.79.Gn, 42.50.Gy DOI: 10.1088/0256-307X/35/3/034201

In recent years, research of single-photon scattering in waveguide systems has attracted a great deal of attention due to their potential applications in quantum information processing and quantum computation.[1−10] Among these scattering properties, Fano resonance[11−16] in the transport spectra is an intriguing feature and is investigated widely in the double-emitter configuration system, and the physical mechanism of the quantum phenomenon is examined, due to the spatial quantum interference between the delocalized and localized channels. Furthermore, with the rapid development of the single-photon transport technique, quantum routing of single photons is demonstrated in various quantum networks,[17−25] where photonic waveguides are served as the quantum channels of the quantum signals, and the quantum routers are utilized to control the propagating paths of the single photons in these channels. However, the Fano-like routing draws relatively less attention in these quantum networks with the single-emitter configuration, due to the limitation of the single-dot construction.

The dipole-dipole interaction (DDI) of two atoms is a common one generated by the coupling of their electric or magnetic dipole moments. Generally, when the relative distance of two atoms is small, the DDI becomes important and cannot be neglected. A number of investigations have been devoted to its practical applications in quantum information processing, such as deterministically creating multiparticle entanglement,[26,27] maintaining the multiqubit entanglement in the dissipative non-Markovian environment,[28,29] optimizing the temporary evolution of quantum discord,[30,31] and implementing the quantum C-Not gate with high fidelity.[32] In addition, many interesting photon scattering properties[33−37] characterized by DDI have also been demonstrated, which include designing the quantum switching, and augmenting the atomic saturation by weakening atomic dissipation and the detuning with the increase of the DDI, etc.

Motivated by the above considerations, we investigate the quantum routing of single photons in a system consisting of two linear waveguides coupled with two collocated atoms, and focus on the Fano-like feature of the four-outport scattering spectra in the single-dot configuration. By adopting a full quantum approach in real space,[3] the reflection and transmission amplitudes of single photons in two waveguide channels are obtained exactly. It has been shown that Fano resonance can be controlled by adjusting the atomic DDI, since DDI provides a delocalized channel[26,33] to enhance the quantum interference. In contrast to previous theoretical schemes concentrating on the double-dot case,[11−16] Fano behavior of the reflection and transmission can emerge in the single-dot configuration with two collocated atoms by controlling the atomic DDI, which may provide another possible way to lead to Fano resonance.

The considered system is illustrated schematically in Fig. 1, where two different two-level atoms are side coupled to the two parallel waveguides. Here the two atoms are assumed to be connected to the photon modes at the same position, which is a valid approximation for a small ensemble of atoms, as the radius of the ensemble is smaller than the resonant radiation wavelength.[38] Since the relative atomic distance is small, the two collocated atoms are also coupled via

*Supported by the National Natural Science Foundation of China under Grant No 11247032, the Natural Science Foundation of Jiangxi Province under Grant Nos 20151BAB202012 and 20151BAB212004, and the Scientific Research Foundation of the Jiangxi Provincial Education Department under Grant No GJJ160633.

**Corresponding author. Email: jshuangjs@126.com

© 2018 Chinese Physical Society and IOP Publishing Ltd

the interatomic dipole-dipole interaction.

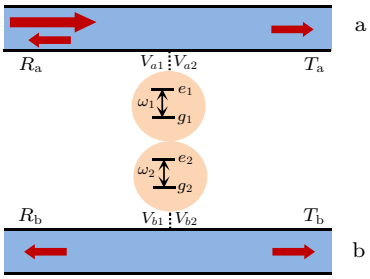


**Fig. 1.** Schematic routing of single photons in two waveguides (labeled as a and b), controlled by two different two-level atoms at the same position. Here $R_a$, $R_b$ and $T_a$, $T_b$ are the reflection and transmission probabilities of the single photons, respectively.

When a single photon is incident from the left of waveguide a, it will propagate or be reflected by the atoms along the four ports of the two waveguide channels, as the system is served as a quantum router. The Hamiltonian describing the composite system can be written as

$$H = H_w + H_a + H_i, \tag{1}$$

where $H_w$ represents the free propagation of the photon in the waveguides, $H_a$ describes the two atoms, and $H_i$ denotes the interaction between the photon and the atoms. For the single-mode waveguide, it can be divided into right- and left-moving modes via the positive and negative momentum photons. As a consequence, $H_w$ can be written as ($\hbar = 1$ throughout this study)

$$H_w = \int dx \Big\{ \sum_{m=a,b} [C^\dagger_{Rm}(x)(\omega_{0m} - iv_g)\frac{\partial}{\partial x} C_{Rm}(x) + C^\dagger_{Lm}(x)(\omega_{0m} + iv_g)\frac{\partial}{\partial x} C_{Lm}(x)] \Big\}, \tag{2}$$

where $\omega_{0m}$ is a reference frequency that is away from the cutoff of the dispersion in the linear waveguide. For simplicity of calculation, we set $\omega_{0a} = \omega_{0b} = \omega_0$, $v_g$ is the group velocity of photons, and $C^\dagger_R(x)$ $[C^\dagger_L(x)]$ denotes the creation operator of a right (left)-traveling photon in the waveguide at position $x$. Within the rotating wave approximation, the atomic Hamiltonian $H_a$ is expressed as

$$H_a = \sum_{n=1,2} (\omega_n - i\frac{\gamma_n}{2})\sigma_{e_n,e_n} + J(\sigma^{(1)}_+\sigma^{(2)}_- + \sigma^{(1)}_-\sigma^{(2)}_+), \tag{3}$$

where we have set the energy scale such that these two ground-state energies are zeros, $\omega_n$ is the circular frequency of energy level $e_n$, $\gamma_n$ is the dissipation rate of the excited state $|e_n\rangle$ of the $n$th atom with $n = 1, 2$, $\sigma_{e_n,e_n} = |e_n\rangle\langle e_n|$ represents the diagonal element, and $\sigma^{(n)}_+ = |e_n\rangle\langle g_n|$ $(\sigma^{(n)}_- = |g_n\rangle\langle e_n|)$ denotes the raising (lowering) operator of the $n$th atom. Here $J$ represents the interatomic dipole-dipole interaction strength, with the mathematical formalism

$$J = \frac{1}{r^3_{12}}\Big[\boldsymbol{d}\cdot\boldsymbol{d} - \frac{3(\boldsymbol{d}\cdot\boldsymbol{r}_{12})^2}{\boldsymbol{r}^2_{12}}\Big], \tag{4}$$

where $\boldsymbol{r}_{12}$ is the relative position between the two atoms, and $\boldsymbol{d}$ is the static electric dipole moment of the atom. The parameter $J$ can also be reduced to the form of $J = \langle e_1, g_2|\boldsymbol{d}|g_1, e_2\rangle$, which means that it can be generated by exchanging the virtual photon in the transition channel of $|e_1\rangle$ and $|e_2\rangle$.

The interaction Hamiltonian $H_i$ is given by

$$H_i = \sum_{m=a,b}^{n=1,2} V_{mn} \int dx\delta(x)[C^\dagger_{Lm}(x)\sigma^{(n)}_- + C^\dagger_{Rm}(x)\sigma^{(n)}_- + \text{H.c.}], \tag{5}$$

where $V_{mn}$ is the coupling between the transition $|e_n\rangle \sim |g_n\rangle$ and the bosonic mode of photons, and $\delta(x)$ indicates that the interaction occurs at $x = 0$.

Assume that the atom is initially in its ground state and the photon is incident from the far left of waveguide a with the linear energy $E_k = \omega_0 + \omega = \omega_0 + v_g k$, where $k$ is the wave vector of the incident photon mode. The scattering eigenstate of the Hamiltonian (1) is then given by

$$|\psi\rangle = \sum_{m=a,b} \int dx[\phi_{Rm}(x)C^\dagger_{Rm}(x) + \phi_{Lm}(x)C^\dagger_{Lm}(x)]|\emptyset_a, \emptyset_b, g_1, g_2\rangle + \xi_1|\emptyset_a, \emptyset_b, e_1, g_2\rangle + \xi_2|\emptyset_a, \emptyset_b, g_1, e_2\rangle, \tag{6}$$

where $\phi_{Rm/Lm}$ is the single photon wave function in the right/left of the waveguide m, $|\emptyset_a, \emptyset_b\rangle$ describes the photonic vacuum, $\xi_1$ and $\xi_2$ are the excitation amplitude of the atomic states. Furthermore, the corresponding wave function can be expressed formally as

$$\begin{aligned}
\phi_{Ra}(x) &= t_a e^{ikx}\theta(x) + e^{ikx}\theta(-x),\\
\phi_{La}(x) &= r_a e^{-ikx}\theta(-x),\\
\phi_{Rb}(x) &= t_b e^{ikx}\theta(x),\\
\phi_{Lb}(x) &= r_b e^{-ikx}\theta(-x),
\end{aligned} \tag{7}$$

where $t_a$ and $r_a$ are the transmission and reflection amplitudes in waveguide a, $t_b$ and $r_b$ are the transmission and reflection amplitudes in waveguide b, respectively, and $\theta(x)$ is the Heaviside step function with $\theta(0) = 1/2$.

By solving the eigen-equation $H|\psi\rangle = E_k|\psi\rangle$, the expressions of $t_a$, $r_a$, $t_b$ and $r_b$ can be obtained as

follows:

$$t_{\rm a} = 1 + \frac{B_1\Gamma_{\rm a2} + B_2\Gamma_{\rm a1} + 2A\sqrt{\Gamma_{\rm a1}\Gamma_{\rm a2}}}{i(B_1B_2 - A^2)},$$
$$r_{\rm a} = \frac{B_1\Gamma_{\rm a2} + B_2\Gamma_{\rm a1} + 2A\sqrt{\Gamma_{\rm a1}\Gamma_{\rm a2}}}{i(B_1B_2 - A^2)},$$
$$t_{\rm b} = r_{\rm b} = \frac{1}{[i(B_1B_2 - A^2)]}\big[B_1\sqrt{\Gamma_{\rm a2}\Gamma_{\rm b2}} + B_2\sqrt{\Gamma_{\rm a1}\Gamma_{\rm b1}} + A(\sqrt{\Gamma_{\rm a1}\Gamma_{\rm b2}} + \sqrt{\Gamma_{\rm b1}\Gamma_{\rm a2}})\big], \quad (8)$$

where $\Gamma_{mn} = V_{mn}^2/v_{\rm g}$, $A = J - i(\sqrt{\Gamma_{\rm a1}\Gamma_{\rm a2}} + \sqrt{\Gamma_{\rm b1}\Gamma_{\rm b2}})$, and $B_n = \omega + \delta_n + i(\Gamma_{\rm an} + \Gamma_{\rm bn} + \gamma_n/2)$, with $\delta_n = \omega_o - \omega_n$.

The quantum routing properties of single photons in the four ports are characterized by the transmission coefficient $T_{\rm a(b)} = |t_{\rm a(b)}|^2$ and the reflection coefficient $R_{\rm a(b)} = |r_{\rm a(b)}|^2$. It can be checked numerically for the relation $T_{\rm a} + R_{\rm a} + T_{\rm b} + R_{\rm b} = 1$ in the non-dissipative case ($\gamma_1 = \gamma_2 = 0$), which means that the transmission and reflection probabilities are conserved. In the single-emitter configuration, the routing probability spectra of single photons have been investigated extensively, while the Fano-like feature does not draw much attention due to the limitation of the single-dot construction. Here we focus on discussing how the atomic DDI influences the Fano behavior of the reflection and transmission.

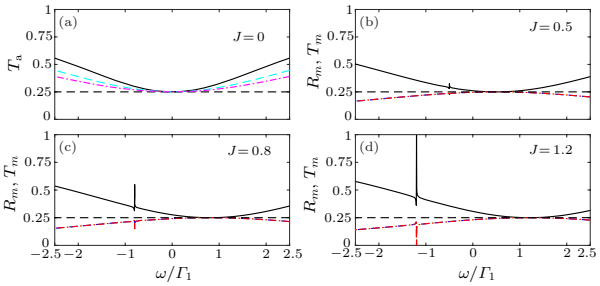


**Fig. 2.** The transmission $T_{\rm a}$ for $\Gamma_2 = 0.5$ (solid black curve), $\Gamma_2 = 1.1$ (dashed cyan curve), and $\Gamma_2 = 1.6$ (dash-dotted pink curve) in (a) $J = 0$. The transmission $T_m$ (solid black $T_{\rm a}$ and dashed blue $T_{\rm b}$), reflection $R_m$ ($R_{\rm a}$ and dash-dotted red $R_{\rm b}$) for different dipole-dipole interaction strengths: (b) $J = 0.5$, (c) $J = 0.8$, and (d) $J = 1.2$. Other parameters are $\gamma_1 = \gamma_2 = 0$, and $\delta_1 = \delta_2 = 0$. Here the curve of $R_{\rm a}$ is covered by the curve of $R_{\rm b}$ due to the relation of $R_{\rm a} = R_{\rm b}$. For convenience, all the parameters are in units of $\Gamma_1$, and $\Gamma_1 = 1$ is set.

For simplicity, the coupling strength between the atom and two waveguides is assumed to be equal, i.e., $\Gamma_{\rm a1} = \Gamma_{\rm b1} = \Gamma_1$ and $\Gamma_{\rm a2} = \Gamma_{\rm b2} = \Gamma_2$, which can be easily achieved to equate the direction of the dipole moment of the atomic exciton and distances between the atom and the parallel waveguides. Figure 2(a) shows the smooth transmission and reflection spectra for different couplings ($\Gamma_2$) at the absence of DDI. When increasing $J$, the Fano resonance occurs and Fano-line shapes in four ports become more evident, as seen in Figs. 2(b)–2(d).

Fano resonance results from the quantum interference between the delocalized and localized channels. When a resonant field is tuned to produce dipole-dipole coupling, a decohering channel (delocalized channel) becomes available because the induced dipoles can spontaneously emit photons and lead to the direct particle transition exchange between $|e_1\rangle$ and $|e_2\rangle$,[26,33] as seen in Eq. (3), while the transition path $|g_n\rangle \Leftrightarrow |e_n\rangle$ through the incident photons provides another channel (localized channel). Therefore, increasing the DDI reinforces the interference between the localized and delocalized channels and leads to more distinct asymmetric line shapes.

Furthermore, the atoms-waveguide coupling can also affect the Fano-like routing in the scattering spectra of single photons. Keeping the interatomic dipole-dipole interaction fixed, Fig. 3 shows the transmission and reflection spectra for different atom-waveguide coupling ratios $\Gamma_2/\Gamma_1$. When increasing $\Gamma_2/\Gamma_1$, the Fano resonance occurs and the Fano-line shapes become more evident as seen in Figs. 3(c) and 3(d). The coupling strength can be controlled by varying the atom-waveguide separation or applying an external field to orient the direction of the dipole moment of the atomic exciton. Thus adjusting the atoms-waveguide coupling strength can provide another way to control effectively the Fano-like routing.

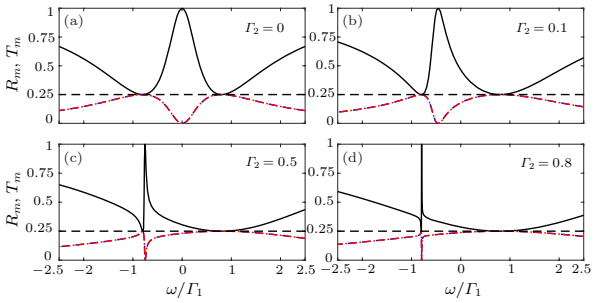


**Fig. 3.** The transmission $T_m$ (solid black $T_{\rm a}$ and dashed blue $T_{\rm b}$), reflection $R_m$ ($R_{\rm a}$ and dash-dotted red $R_{\rm b}$) for different coupling strength ratios: (a) $\Gamma_2 = 0$, (b) $\Gamma_2 = 0.1$, (c) $\Gamma_2 = 0.5$, (d) $\Gamma_2 = 0.8$. The other parameters are $\gamma_1 = \gamma_2 = 0$, and $\delta_1 = \delta_2 = 0$, and $J = 0.8$. Here the curve of $R_{\rm a}$ is covered by the curve of $R_{\rm b}$ due to the relation of $R_{\rm a} = R_{\rm b}$. These parameters are in units of $\Gamma_1$.

To investigate the influence of the detuning $\delta_n$ on the Fano-like resonance, Fig. 4 displays the transmission $T_{\rm a}$ as a function of $\omega/\Gamma_1$ under the dipole-dipole interaction strength $J = 0$ and $J = 0.8\Gamma_1$. When the dipole-dipole interaction is of absence, the spectra is smooth or one peak is exhibited for three kinds of detunings, such as $\delta_1 = \delta_2 = 0.5\Gamma_1$, $\delta_1 = \delta_2 = -0.5\Gamma_1$, and $\delta_1 = -\delta_2 = -0.5\Gamma_1$. Interestingly, the Fano-line shapes appear in the case of the negative detuning $\delta_1$ and positive detuning $\delta_2$ under the condition $J = 0.8\Gamma_1$, as plotted in Fig. 4(c). Note that the dissipations are not considered in the above investigations. In real experiments, the atom-waveguide system inevitably experiences dissipations, such as the

atomic excited-state relaxation and photon loss, since it is also coupled to the environment. As shown in Figs. 4(b) and 4(d), the dissipations are included and result in lower probability of scattering coefficients, but the Fano-resonance feature remains similar. Therefore, the influence of the dissipations to the Fano-like routing properties should not be dominant.

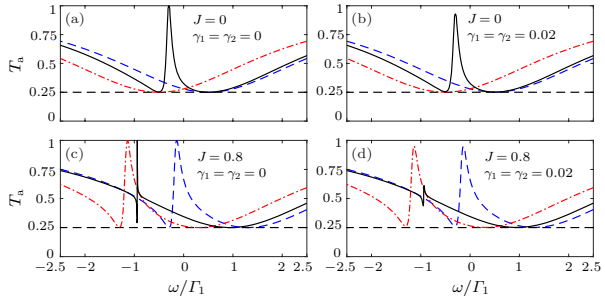


**Fig. 4.** Transmission $T_a$ as a function of $\omega/\Gamma_1$ for different detunings: $\delta_1 = \delta_2 = 0.5$ (dash dotted red), $\delta_1 = \delta_2 = -0.5$ (dashed blue), and $\delta_1 = -\delta_2 = -0.5$ (solid black); (a) and (b) with $J = 0$, (c) and (d) with $J = 0.8$, and (b) and (d) with $\gamma_1 = \gamma_2 = 0.02$. These parameters are in units of $\Gamma_1$.

Note that the routing of single photons in one waveguide can be performed. Efficient single-photon routing is demonstrated in a fiber waveguide coupled to a toroidal cavity,[18] where duplex signal transmission works effectively in the waveguide channel and the compact interaction between the toroidal cavity, and only a waveguide field mode is obtained. Here our scheme is discussed in two waveguide channels, in which all-optical routing of four output ports is also examined, and the quantum signal distractions are excluded.[23–25] Single-photon routing in the two-waveguide channel of our scheme can be controlled by adjusting the waveguide atom couplings and the atomic dipole-dipole interaction. It is not easy to modulate these parameters for natural atoms, while artificial atoms in the transmission line waveguides can be taken into account as an alternative.

Remarks on the validity of our discussions for the practicable system and experimental parameters should be given. The system can be constructed by two microwave transmission line waveguides, in which single-photon quantum routing by two distant artificial atoms has been demonstrated by Chen *et al.*,[23] and their results show that high routing transfer can be controlled by varying the detuning of the atoms and the interatomic distance. Here we focus on two adjacent atoms, it can be operated by closely locating two transmon qubits (optimized Cooper-pair boxes) at an antinode of the microwave field in the half-wave resonator ($L = \lambda/2 = 12.3\,\text{mm}$).[39] In the numerical calculations, the choices of these parameters are close to the experimental results in the circuit QED systems.[39,40] These parameters are taken as $\Gamma_1 = 2\pi\times6.73\,\text{MHz}$, $J = 2\pi\times13\,\text{MHz}$, $\omega_1 = 2\pi\times6.469\,\text{GHz}$, $\omega_2 = 2\pi\times6.546\,\text{GHz}$, and $\gamma_1 = \gamma_2 = 2\pi\times0.02\,\text{MHz}$. Experimentally, in the circuit QED system, the ultrastrongly coupling strength between the superconducting flux qubit and the microwave field can be easily modulated by applying an external flux bias to the circuit loop,[41,42] while the inter-qubit interaction from the virtual exchange of microwave photons with the cavity, which is similar to the atomic dipole-dipole interaction, can be conveniently tuned by adjusting the detunings between qubits and resonator.[39] As the coupling strengths $V/2\pi$ between 5.8 and 100 MHz can be modulated experimentally,[40] all the parameters scaled by the reduced atom-waveguide coupling $\Gamma_1$ in the above numerical calculations are available.

Signal input and readout in four ports should also be mentioned here. The input photon is separated from the output signal by an optical circulator, and thus the single photon can be directed into the waveguide channel completely.[23–25] In each port, a 50/50 beam splitter followed by two single-photon counting modules (SPCMs) is connected to detect the output field. Photoelectric events from these SPCMs are stamped and recorded for analysis.[18,24] With these setups, the transmission and reflection spectra of microwave photons can be measured by scanning the frequency spectra of the incident photons.

In conclusion, we focus on the Fano-like feature of the single-photon quantum routing in a waveguide network with a small ensemble of atoms. With a full quantum theory in real space, the scattering amplitudes are analytically obtained, and the Fano-like transport is discussed in detail. It is found that, evident Fano-line shapes are revealed in the scattering spectra of the single-dot configuration system, by adjusting the atomic DDI. Moreover, Fano-like routing can also be controlled by adjusting the atom-waveguide coupling strength ratio and the detuning of atoms, under the condition of the presence of the atomic DDI. Therefore, the proposed system may provide potential applications in controlling quantum Fano-like resonance.

## References

[1] Shen J T and Fan S 2005 *Phys. Rev. Lett.* **95** 213001
[2] Chang D E, Sørensen A S, Demler E A and Lukin M D 2007 *Nat. Phys.* **3** 807
[3] Shen J S and Fan S 2009 *Phys. Rev.* A **79** 023837
[4] Zhou L, Gong Z R, Liu Y X, Sun C P and Nori F 2008 *Phys. Rev. Lett.* **101** 100501
[5] Shi T and Sun C P 2009 *Phys. Rev.* B **79** 205111
[6] Yan C H, Wei L F, Jia W Z and Shen J T 2011 *Phys. Rev.* A **84** 045801
[7] Cheng M T, Luo Y Q, Wang P Z and Zhao G X 2010 *Appl. Phys. Lett.* **97** 191903
[8] Cheng M T, Song Y Y and Yu L B 2012 *Chin. Phys. Lett.* **29** 054211
[9] Cheng M T, Ye G L, Zong W W and Ma X S 2016 *Chin. Phys. Lett.* **33** 024205
[10] Zhang X Q, Xia X W, Xu J P and Yang Y P 2017 *Chin.*

*Phys.* B **26** 054208
[11] Chen W, Chen G Y and Chen Y N 2011 *Opt. Lett.* **36** 3602
[12] Chen G Y and Chen Y N 2012 *Opt. Lett.* **37** 4023
[13] Chen W, Chen G Y and Chen Y N 2010 *Opt. Lett.* **18** 10360
[14] Chen G Y, Liu M H and Chen Y N 2014 *Phys. Rev.* A **89** 053802
[15] Cheng Y, Tan Z, Wang J, Zhu Y F and Zhan M S 2016 *Chin. Phys. Lett.* **33** 014202
[16] Huang M, Chen D, Zhang L and Zhou J 2016 *Chin. Phys.* B **25** 057303
[17] Xia K and Twamley J 2013 *Phys. Rev.* X **3** 031013
[18] Aoki T, Parkins A S, Alton D J, Regal C A, Dayan B, Ostby E, Vahala K J and Kimble H J 2009 *Phys. Rev. Lett.* **102** 083601
[19] Hoi I C, Wilson C M, Johansson G, Palomaki T, Peropadre B and Delsing P 2011 *Phys. Rev. Lett.* **107** 073601
[20] Zhou L, Yang L P, Li Y and Sun C P 2013 *Phys. Rev. Lett.* **111** 103604
[21] Lu J, Zhou L, Kuang L M and Nori F 2014 *Phys. Rev.* A **89** 013805
[22] Lemr K, Bartkiewicz K, Černoch A and Soubusta J 2013 *Phys. Rev.* A **87** 062333
[23] Chen X Y, Zhang F Y and Li C 2016 *J. Opt. Soc. Am.* B **33** 583
[24] Yan W B and Fan H 2014 *Sci. Rep.* **4** 4820
[25] Yan W B, Liu B, Zhou L and Fan H 2015 *Europhys. Lett.* **111** 64005
[26] Brennen G K, Deutsch I H and Jessen P S 2000 *Phys. Rev.* A **61** 062309
[27] Zhang X L, Isenhower L, Gill A T, Walker T G and Saffman M 2010 *Phys. Rev.* A **82** 030306
[28] Li Y, Zhou J and Guo H 2009 *Phys. Rev.* A **79** 012309
[29] An N B, Kim J and Kim K 2011 *Phys. Rev.* A **84** 022329
[30] Berrada K, Fanchini F F and Khalek S A 2012 *Phys. Rev.* A **85** 052315
[31] Susa C E and Reina J H 2012 *Phys. Rev.* A **85** 022111
[32] Isenhower L, Urban E, Zhang X L, Gill A T, Henage T, Johnson T A, Walker T G and Saffman M 2010 *Phys. Rev. Lett.* **104** 010503
[33] Yu X Y and Li J H 2013 *Eur. Phys. J.* D **67** 177
[34] Zhang Y Q, Tan L and Barker P 2014 *Phys. Rev.* A **89** 043838
[35] Cheng M T, Ma X S and Wang X 2014 *Chin. Phys. Lett.* **31** 014202
[36] Xu D, Wang X Y, Gang Y, Ouyang S L, He H L and He H 2015 *Chin. Phys.* B **24** 024205
[37] Meng T F, Ji Z H, Zhao Y T, Xiao L T and Jia S T 2016 *Chin. Phys. Lett.* **33** 113202
[38] Roy D 2013 *Phys. Rev.* A **87** 063819
[39] Majer J, Chow J M, Gambetta J M, Koch J, Johnson B R, Schreier J A, Frunzio L, Schuster D I, Houck A A, Wallraff A, Blais A, Devoret M H, Girvin S M and Schoelkopf R J 2007 *Nature* **449** 443
[40] Blais A, Gambetta J, Wallraff A, Schuster D I, Girvin S M and Devoret M H 2007 *Phys. Rev.* A **75** 032329
[41] Peropadre B, Forn-Díaz P, Solano E and García-Ripoll J J 2010 *Phys. Rev. Lett.* **105** 023601
[42] Richer S, Maleeva N, Skacel S T, Pop I M and DiVincenzo D 2017 *Phys. Rev.* B **96** 174520